Heliyon 7 (2021) e06481

Contents lists available at ScienceDirect

Heliyon

journal homepage: www.cell.com/heliyon

Research article

Advanced design and manufacturing of custom orthotics insoles based on hybrid Taguchi-response surface method

P.W. Anggoro [a,*], B. Bawono [a], J. Jamari [b], M. Tauviqirrahman [b], A.P. Bayuseno [b]

[a] Department of Industrial Engineering, Faculty of Industrial Technology, University of Atma Jaya Yogyakarta, Jl. Babarsari 44, Yogyakarta 55281, Indonesia
[b] Department of Mechanical Engineering, University of Diponegoro, Jl. Prof. Soedarto, SH., Tembalang, Semarang 50275, Indonesia

ARTICLE INFO

Keywords:
EVA foam
CNC milling
RSM
Taguchi method
Surface roughness
Optimization

ABSTRACT

Herein, a machining strategy to fabricate custom orthotic insoles with high surface finish and wide fit tolerance is presented. CNC milling was used to machine ethylene-vinyl acetate (EVA) foam for insoles with various surface hardness, and the Taguchi-response surface method (TM-RSM) was adopted to optimize the parameters of the CNC milling process (cutting speed, feed rate, tool path strategy, and step over). EVA foam with varying surface hardness and the tolerance of the wide fit insoles corresponding to the surface roughness were analyzed. Subsequently, a mathematical model was established to determine the optimal CNC milling parameters for a standard milling cutter under dry coolants. The results of the six parameters corresponding to the mean values of surface roughness were initially examined using the signal-to-noise ratio of the Taguchi method (TM). The surface roughness obtained with the TM-RSM was up to 4.13% higher than that obtained with the TM. The EVA foam insole with a surface hardness of 50–60 HRC and a wide fit tolerance of 0.75 mm provided the ideal level of comfort and support for patients with diabetes. The results of this study demonstrated that CNC milling provided a better surface finish of orthotic shoe insoles than other methods, which can serve as guidance in the development of machining strategies for insoles made from EVA foam.

1. Introduction

Ethylene-vinyl acetate (EVA) foam has many applications in sports and medicine owing to its excellent properties relative to those of other polymers, including good energy absorption capacity and high-fracture toughness (Shimazaki et al., 2016). In sports applications, EVA foam is typically layered with harder polymers, such as polycarbonate and composite laminates, to provide damping. In the footwear industry sector, EVA foam is mostly used in orthotic shoe insoles because it helps realize lightweight shoes with high comfort, resiliency, and durability (Shimazaki et al., 2016).

In the last decade, foot orthotics insoles with EVA foam have been proposed for the effective treatment of foot pain (Hawke et al., 2008) and foot ulcers, which are commonly experienced by diabetic patients (Boulton et al., 2004; Ghassemi et al., 2015). Specifically, foot ulcers are the main cause of foot infections, which can lead to foot amputation. Diabetic patients are susceptible to foot ulcers and foot pain (Matricali et al., 2007). However, diabetic patients' foot ulcers and foot pain can be treated by wearing custom-made insoles, which can reduce the mechanical load on the plantar foot ulceration during walking (Landorf et al., 2001; Dombroski et al., 2014; Anggoro et al., 2017). Custom-made insoles with good comfort and support can help prevent pain in the foot. For this purpose, the product design, surface hardness of EVA foam, and wide fit profile of orthotic insoles are the primary factors influencing the foot-insole interface pressures, comfort during walking, and, eventually, effective foot orthotics treatment (Qiu et al., 2011).

In fact, the surface characteristics of an insole, namely the hardness and roughness, may affect the perception and biomechanical surface contact experienced by the foot of a diabetic patient under the influence of shock and impact loads. Additionally, the dimensional matching of a shoe profile with a patient's foot size has a strong influence on the reduction of foot pain. These requirements of the surface quality and custom-fitting can be met through the product design of orthotic shoe insoles and the appropriate manufacturing process, which must achieve high surface quality, wide fits, and production efficiency (Berry et al., 2013).

Nowadays, orthotic insoles can be ordered and made using footprints in a foam box. Nevertheless, this method often has low precision and accuracy of the insole when assembled with the patient's foot geometry and frequently produces orthotic footwear with low comfort. Moreover, this traditional method often leads to higher costs and production time

* Corresponding author.
E-mail address: pauluswisnuanggoro@ymail.com (P.W. Anggoro).

https://doi.org/10.1016/j.heliyon.2021.e06481
Received 26 September 2019; Received in revised form 17 December 2019; Accepted 3 March 2021

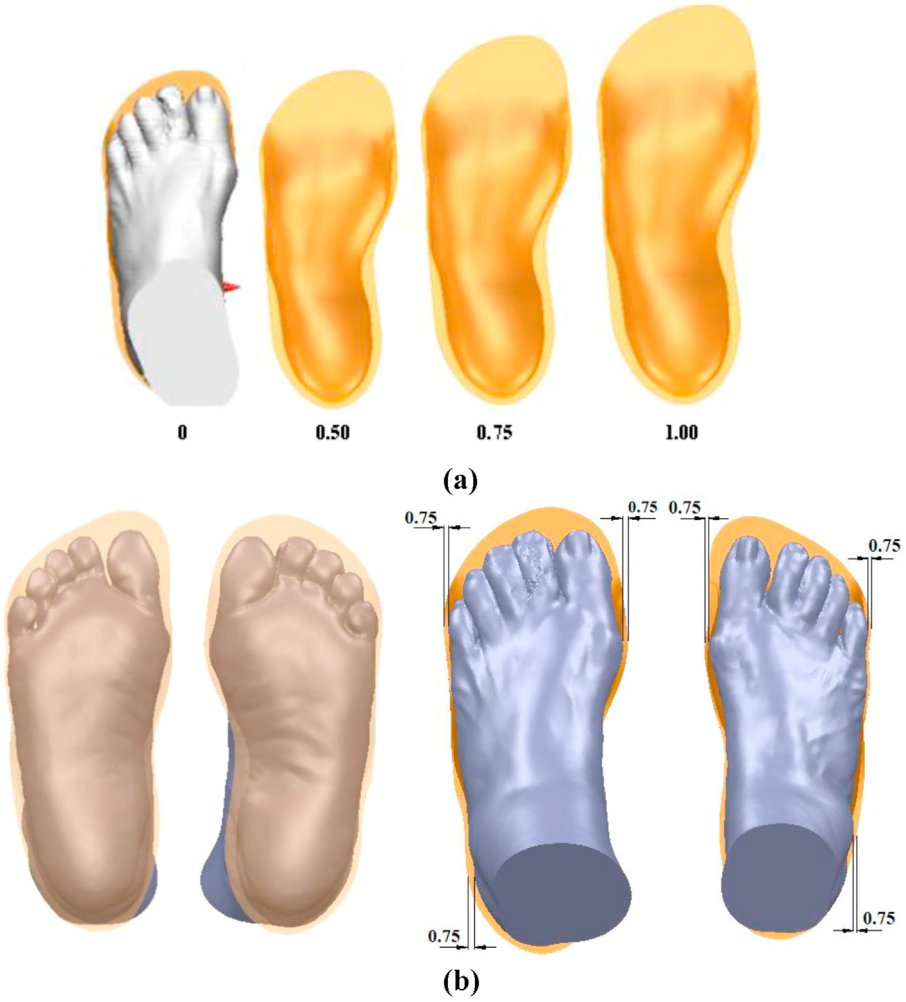

Figure 1. 3D CAD model of custom orthotics insoles: (a) variation in wide fit tolerance of insoles along X and Y axes; (b) top view of the insole with 0.75 mm width fit tolerance and 3D physical model of the foot base in contact with the insole.

(Vicenzino, 2004). With the rapidly developing computer-aided design (CAD) technology, three-dimensional (3D) design of orthotic insoles can be made for various foot contours with optimal fit and minimum production cost and design time (Ye et al., 2008). Additionally, reverse engineering and reverse innovative design (RID) allow the rapid production of insoles with highly accurate and precise size (Dombroski et al., 2014; Jeng et al., 2012; Xia, 2014). Practically, the contour of foot abnormalities can be scanned by a 3D scanner providing accurate 3D data, which can subsequently be used in a subtractive manufacturing process of insoles (either adaptive manufacturing using a 3D printer or a CNC milling machine) (Munro, 2005; Li et al., 2017).

3D-foot scanning system, CAD, and computer-aided manufacturing (CAM) have become suitable and cost-effective for the fabrication of molds and custom-made orthotics insoles (Dombroski et al., 2014; Salles and Gyi, 2013). Various insole designs can be fabricated according to the requirements of the feet of diabetic patients. 3D printing has been applied in the CAM of an ankle-foot orthotic (AFO) shoes with high dimensional accuracy (Creylman et al., 2013; Faustini et al., 2008; Schrank et al., 2013) and has been shows to produce orthotic insoles with a good fit for foot patients with diabetes (Dombroski et al., 2014; Salles and Gyi, 2012, 2013; Pallari et al., 2010). 3D footprints made of polymeric materials need to be further strengthened by a machining strategy to improve their surface roughness.

As a machining strategy, CNC milling offers pieces (unit) or a smaller production process and has been shown to enable the simple and scalable fabrication of insoles with good fits. However, the machining of EVA foam for use in orthotic insoles is a challenging process because the material has anisotropic and non-homogeneous properties (Shimazaki et al., 2016). Unlike metal machining, the machining of EVA foam is susceptible to compressive shearing and fracture phenomena. Therefore, there are stringent requirements with respect to the selection of machining parameters and the surface hardness of the material.

In fact, the surface quality (surface roughness) of custom-made insoles must be high for the effective offloading of the foot and anticipation of foot ulcers depending on the hardness of the surface material and dimensional accuracy of the profile shoes. It is also known that these characteristics are strongly dependent on the machining process undergone by the material. However, most related studies (Xavior and Adithan, 2009; Hanafi et al., 2012; Asiltürk and Nesseli, 2012; Sarıkaya and Güllü, 2014; Yadav, 2017) investigated the process parameters in the turning process of a rubber-based product, but no findings have been published on the CNC machining of EVA foam with varied surface hardness. In addition, most previous studies on CNC milling have focused on the determination of optimal parameters with respect to a flat surface (Sait et al., 2009; Anggoro et al., 2016, 2017, 2018, 2019a, 2019b, 2019c; Chabbi et al., 2017; Bawono et al., 2019).

In this study, CNC milling of EVA foam with varied surface hardness was performed to determine the surface quality data of the insole product, which can be characterized by the perception and biomechanical variables related to pain prevention and comfort. To the best of the authors' knowledge, this is the first study to explore and combine experimental and modeling approaches for manufacturing rubber-based products with CNC

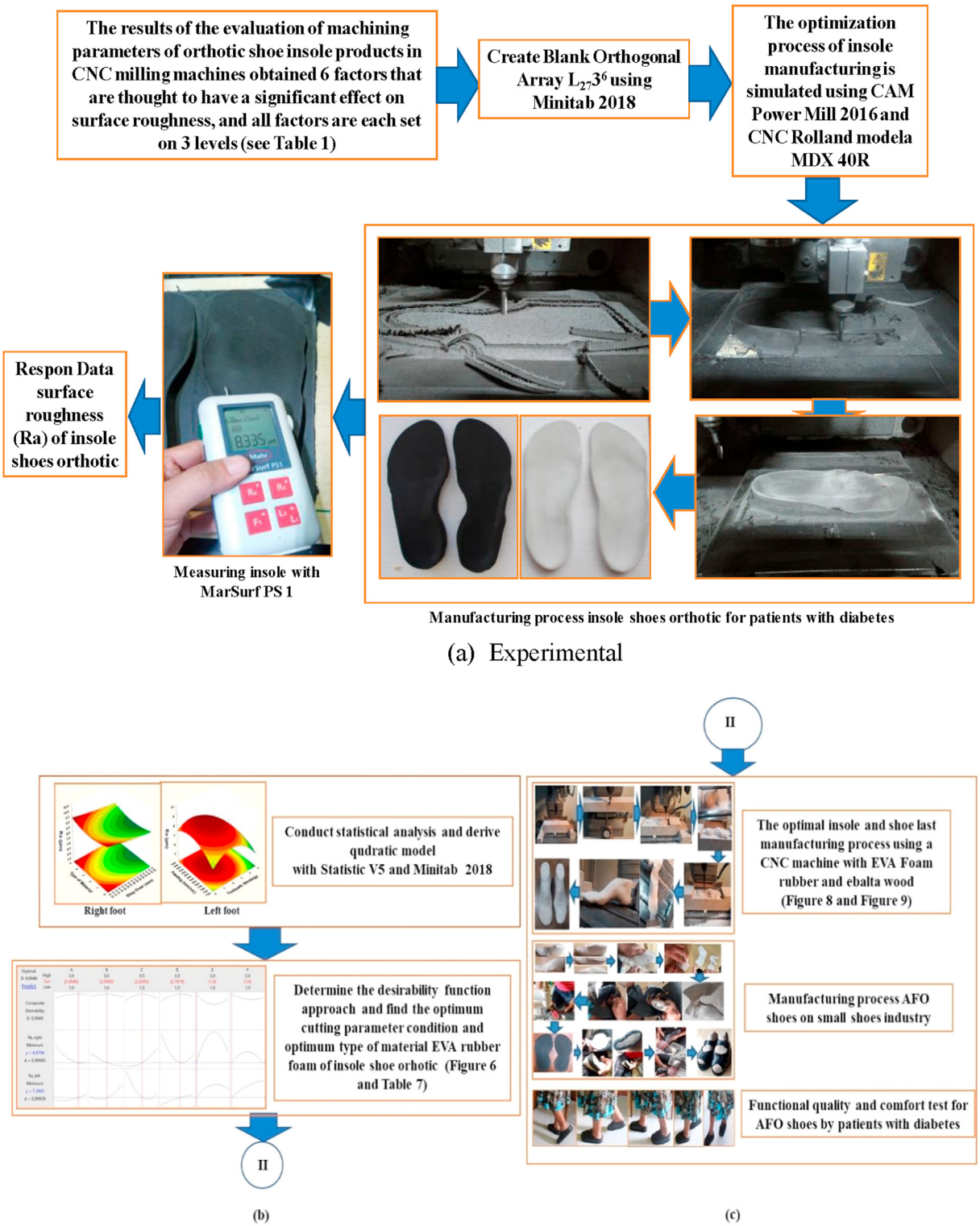

Figure 2. Outline of this research: (a) experiments; (b) modeling; (c) manufacturing of AFO shoes for patients with diabetes.

milling. The objective of this study was to experimentally investigate the process parameters that can achieve the desired surface roughness and generate a mathematical model and process parameter optimization strategy (spindle speed, tool path strategy, feed rate, step over, EVA foam with variable surface hardness, and typical design of insoles with a wider fit tolerance) using the hybrid approach of the Taguchi-response surface method (TM-RSM). This hybrid approach was used to establish the mathematical model and optimize the CNC milling parameters. Finally, the optimal parameters, hardness of the EVA foam, and design of insoles with wide tolerance were determined using a second-order regression model and were plotted against the response data.

2. Materials and methods

2.1. 3D design of orthotic insoles

Three types of orthotic insoles were designed to fit the contour of a diabetic patient's foot. These insoles were subsequently fabricated

Figure 3. Research output: (a) produced EVA foam insoles with different hardness; (b) validation of the insole product with 3D prototype foot and shoe for a patient with diabetes; (c) three types of produced AFO shoes.

through CNC milling. The RID method was used to develop 3D models of insoles using 3D scanning data, of which the base curve surface modeling of three insoles could be explored using the software (PowerSHAPE 2016) according to (Ye et al., 2008; Anggoro et al., 2017, 2018). Figure 1 shows the design results of the insoles with wide fit tolerance (0.50, 0.750, and 1.00 mm). From the figure, it is evident that the RID technique provided an insole model with good dimensional accuracy.

2.2. Workpiece materials, machine tools, and cutting tool specifications

EVA foam with dimensions of 250 × 95 × 23 mm^3 in thickness were machined in the CNC milling experiments. The surface hardness of the material measured using a shore hardness tester (Asker CL-150) was in the range of 20–60 HRC. In the experiment, three types of EVA foams were identified according to the level of hardness: 20–35 HRC (level 1), 35–45 HRC (level 2), and 50–60 HRC (level 3). Based on the price data of EVA foam in the local market of Jakarta, Indonesia, the prices of materials with a size of 1200 × 2400 × 30 mm^3 are as follows: $31.00/sheet (EVA foam with variable surface hardness, level 1), $37.00/sheet (EVA foam with variable surface hardness, level 2), and $47.00/sheet (EVA foam with variable surface hardness, level 3). In general, EVA foam has a density of 55–65 kg/m^3, nominal size of 2000 × 1000 mm^2, split-thickness of 3–36 mm, tensile strength of 800 kPa, and tear strength of 4.5 kN/m (Nurit et al., 2006).

The CNC milling of EVA foam was performed with a milling machine (Rolland Modella MDX40R CNC) with a maximum spindle rotation of 16000 rpm equipped with a brushless DC motor with a power of 100 W. The cutting tool used a carbide tool with the type of end milling [SECO, with specification 93060F] and ball-nose of cutter milling [JS533060D1B0Z3-NXT]. The surface roughness (Ra) was measured with a MarSurf PS1 with a tolerance of 0.001 mm, which provided three cutoffs. The cutoff determined elements of the measured profile associated with roughness. In accordance with ISO, JIS, or ANSI/ASME, the length of the track calculated from the cut off was 5.600 mm, which refers to the cutoff of the decision table according to DIN EN ISO 4288 and has been set on the tester before measuring. The surface roughness of each insole was measured three times on the heel of the foot. The average Ra (left- and right-foot insoles) for each machining experiment are given in Table 3. The stages of this research are presented in Figure 2, and insoles produced are shown in Figure 3.

2.3. Experimental design of machining parameters

The CNC milling parameters, namely the path strategy (Factor A), cutting speed (Factor A), feed rate (Factor C), step over (Factor D), EVA foam with variable surface hardness (Factor E), and the size tolerance in a wide fit orthotic insole (Factor F) were evaluated. These parameters were then designated as their levels for analysis of significant factors in the CNC milling process (Table 1). The experimental design consisted in the tuning of six parameters and three levels selected according to Taguchi's $L_{27}3^6$ of orthogonal arrays, as shown in Tables 2 and 3. In the Taguchi method (TM), the orthogonal array matrix was designed to minimize the number of experiments. The TM also used the signal-to-noise (S/N) ratio to XXXodelli the effects of contributing factors on the yield responses. The characteristics of three S/N ratios were presented as the following concepts: "the smaller the better" (STB), the "highest is the best" and the "highest nominal is the best" and were selected in the process parameter optimization. In the machining experiments, the arithmetic mean of the

Table 1. Parameters of machining and level experiment.

Factor	Level		
	1	2	3
A	Raster	Raster 45°	Step and Shallow
B	14000 rpm	14500 rpm	15000 rpm
C	800 mm/min	850 mm/min	900 mm/min
D	0.20 mm	0.25 mm	0.30 mm
E	20–35 HRC	40–50 HRC	>50 HRC
	($31/sheet)	($37/sheet)	($47/sheet)
F	0.50 mm	0.75 mm	1.00 mm

Table 2. Design matrix of orthogonal array $L_{27}3^6$ for the experimental runs.

Trial number	Factor A	Factor B	Factor C	Factor D	Factor E	Factor F
1	1	1	1	1	1	1
2	1	1	1	1	2	2
3	1	1	1	1	3	3
4	1	2	2	2	1	1
5	1	2	2	2	2	2
6	1	2	2	2	3	3
7	1	3	3	3	1	1
8	1	3	3	3	2	2
9	1	3	3	3	3	3
10	2	1	2	3	1	2
11	2	1	2	3	2	3
12	2	1	2	3	3	1
13	2	2	3	1	1	2
14	2	2	3	1	2	3
15	2	2	3	1	3	1
16	2	3	1	2	1	2
17	2	3	1	2	2	3
18	2	3	1	2	3	1
19	3	1	3	2	1	3
20	3	1	3	2	2	1
21	3	1	3	2	3	2
22	3	2	1	3	1	3
23	3	2	1	3	2	1
24	3	2	1	3	3	2
25	3	3	2	1	1	3
26	3	3	2	1	2	1
27	3	3	2	1	3	2

Ra and the average of the maximum value of the profile (Rz) in the yield of the optimal conditions were calculated using the S/N ratio (Roy, 1990; Montgomery, 2013; Sarıkaya and Güllü, 2014):

$$S \Big/ N \ ratio = -10.log\frac{1}{n}\left(y_1{}^2 + y_2{}^2 + y_3{}^2 + \ldots + y_n{}^2\right) \quad (1)$$

$$S \Big/ N \ ratio(dB) = \left(\frac{average, \mu}{deviation, \acute{\upsilon}}\right)^2, \quad (2)$$

where the variables y_1, y_2, y_3, and y_n are the yield responses of the machining process for a test condition repeated n times. The S/N ratios were calculated using Eqs. (1) and (2) for 27 experimental trials, and their results are listed in Table 4.

In the simulation, the parameters consisted of six factors (A–F) and three treatments. Thus, $3^6 = 729$ experimental trials were conducted. However, the TM reduced the number of treatments and resulted in 27 trials. The experimental outcomes of the 27 trials and the mean values of the surface roughness of the orthotic shoe insoles were calculated, and the surface roughness of the materials was measured using a surface roughness tester (Mark Surf PS 1). The Ra value was obtained from experiments based on selecting the cutting parameters of the CNC machine. The results are presented in Table 3.

The yield responses of the surface roughness, including the S/N ratios, and the effects of the mean surface roughness are presented in Table 4. The effect of each level of the factors on the quality characteristics was using the S/N ratio. The values of each factor (bold) were obtained from the Taguchi quality characteristic formula according to the STB criteria. Accordingly, the smallest Ra value can be achieved if the optimal machining conditions for the left-foot insole experiments are met under the cutting parameter conditions set at level 2 for the toolpath strategy (A), spindle speed (B), feed rate (C), step over (D), type of design insole (F), and hardness of EVA (E) set at level 1. The smallest Ra value for the right-foot insole experiments can be achieved if the cutting parameter conditions are set at level 1 for the feed rate (C) and hardness of EVA (E); level 2 for the toolpath strategy (A), step over (D), and type of design insole (F); and level 3 for the spindle speed (B).

The patients gave written consent to use the data collected during scanning, design, fabrication, and testing of the shoes. It is noted that the ethical approval according to Ethical Clearance No. 27/EC/KEPK/FK.UNDIP/II/2021 was approved by Prof. Dr. dr. Banundari Rachmawati, Sp.PK(K), and confirming that informed consent was obtained from all patients for our experiments.

2.4. Response surface method analysis of the yield response

The response surface method (RSM) is a combination of statistical and mathematical procedures that utilize system modeling and problem analysis to create a response of interest. This response is affected by several variables and the target value (Myers et al., 2009). The first stage of the RSM involves estimating the true function between the "y" value and the set of the independent variable (x_i). When a linear function is obtained, the approximating function is the following first-order model:

$$y = \beta_0 + \beta_1 x_1 + \beta_2 x_2 + \ldots + \beta_k x_k + \varepsilon, \quad (3)$$

where β_0 is a constant, β_k is a regression coefficient, x_1 are input parameters, $\alpha\nu\delta\varepsilon$ is the error.

However, the polynomial function of the second-order model typically recommended because the first-order model has the highest lack-of-fit. Here, the second-order RSM model can be expressed as

$$y = \beta_0 + \sum_{i=1}^{k}\beta_i x_i + \sum_{i=1}^{k}\beta_{ii}x_i^2 + \sum\sum_{i<j}^{\infty}\beta_{ij}x_i x_j + \varepsilon. \quad (4)$$

In this study, the value of each coefficient and constant was computed

Table 3. Surface roughness (Ra) of the left- and right-foot insoles.

Trial number	Uncoded value of the factor						Ra left-foot insole μm	Ra right-foot insole μm
	A	B	C	D	E	F		
1	1	1	1	1	1	1	7,897	8,709
2	1	1	1	1	2	2	9,221	9,551
3	1	1	1	1	3	3	9,478	8,196
4	1	2	2	2	1	1	7,195	7,831
5	1	2	2	2	2	2	8,237	8,915
6	1	2	2	2	3	3	8,668	6,733
7	1	3	3	3	1	1	8,038	8,142
8	1	3	3	3	2	2	8,550	9,401
9	1	3	3	3	3	3	8,753	8,434
10	2	1	2	3	1	2	7,388	7,996
11	2	1	2	3	2	3	8,424	9,340
12	**2**	**1**	**2**	**3**	**3**	**1**	**8,080**	**7,476**
13	2	2	3	1	1	2	8,193	8,510
14	2	2	3	1	2	3	9,556	8,886
15	2	2	3	1	3	1	7,885	9,012
16	2	3	1	2	1	2	8,658	7,672
17	2	3	1	2	2	3	8,160	7,611
18	2	3	1	2	3	1	8,643	7,005
19	3	1	3	2	1	3	8,189	8,266
20	3	1	3	2	2	1	8,814	9,176
21	3	1	3	2	3	2	9,048	8,085
22	3	2	1	3	1	3	8,391	8,098
23	3	2	1	3	2	1	8,200	7,996
24	3	2	1	3	3	2	7,780	8,162
25	3	3	2	1	1	3	8,235	7,085
26	3	3	2	1	2	1	7,825	8,939
27	3	3	2	1	3	2	8,598	9,158

Table 4. Response value for S/N ratios (dB) and means of effect.

Control factor	Surface roughness Ra (left-foot insole)					Surface roughness Ra (right-foot insole)				
	Level 1	Level 2	Level 3	S/N Ra	Delta	Level 1	Level 2	Level 3	S/N Ra	Delta
	Mean (μm)			(dB)	(μm)				(dB)	(μm)
A	8.449	**8.332**	8.342	−18.440	0.11	8.435	**8.168**	8.329	18.357	0.267
B	8.504	**8.234**	8.384	−18.440	0.28	8.548	8.238	**8.146**	18.357	0.402
C	8.492	**8.072**	8.558	−18.437	0.51	**8.096**	8.179	8.657	18.357	0.561
D	8.543	**8.178**	8.401	−18.440	0.36	8.672	**7.907**	8.353	18.357	0.765
E	**8.020**	8.554	8.548	−18.440	0.56	**8.044**	8.853	8.304	18.357	0.819
F	8.408	**8.064**	8.650	−18.443	0.61	8.269	**8.507**	8.606	18.357	0.548

using the least-squares method. Finally, the desirability function (dF) can be used to optimize the multiple-response in the hybrid TM-RSM (Hanafi et al., 2012).

3. Results and discussion

The EVA foam was machined in eight steps. The first step involved the S/N ratio analysis of the data. Noise is introduced by the external environment so the parameter settings varied in the results of the measurements for the Ra of the left- and right-foot insoles. The results of this analysis correspond to the statistical analysis value that has been set with criteria on the smallest S/N ratio, which means that the setting value provided the best/optimal condition (Table 3). The second step involved a graph analysis of each parameter setting to minimize the Ra value (Figure 4). The third step involved a multi-regression analysis to determine the relationship of each variable setting parameter with the Ra value for the left and right feet (Eqs. (4) and (5)). The fourth step involved the testing of the optimal values with the minimum confidence level analysis (less than 5%), and the fifth step involved the analysis of the influence of each factor on the parameter settings to sort the largest to smallest starting influence. The sixth step involved the plotting of each factor in the set parameters against the roughness Ra (Figure 5). The seventh step involved an error analysis based on the TM and hybrid TM-RSM (Tables 7 and 8). The eighth step involved the determination of the optimal parameters employed for designing and producing the AFO shoes. To assess the fit of the shoe products, the DM patients were asked to wear AFO shoes for four weeks and then answer a questionnaire.

In the TM, the S/N ratio was used for analysis of variance (ANOVA) calculations. This ratio was useful for identifying and analyzing scaling factors because the mean and standard deviation of the Ra for the left- and right-foot insoles may vary proportionally. Based on these factors, under the same parameter settings, the results obtained using different roughness values were analyzed by ANOVA for a value parameter setting dominance.

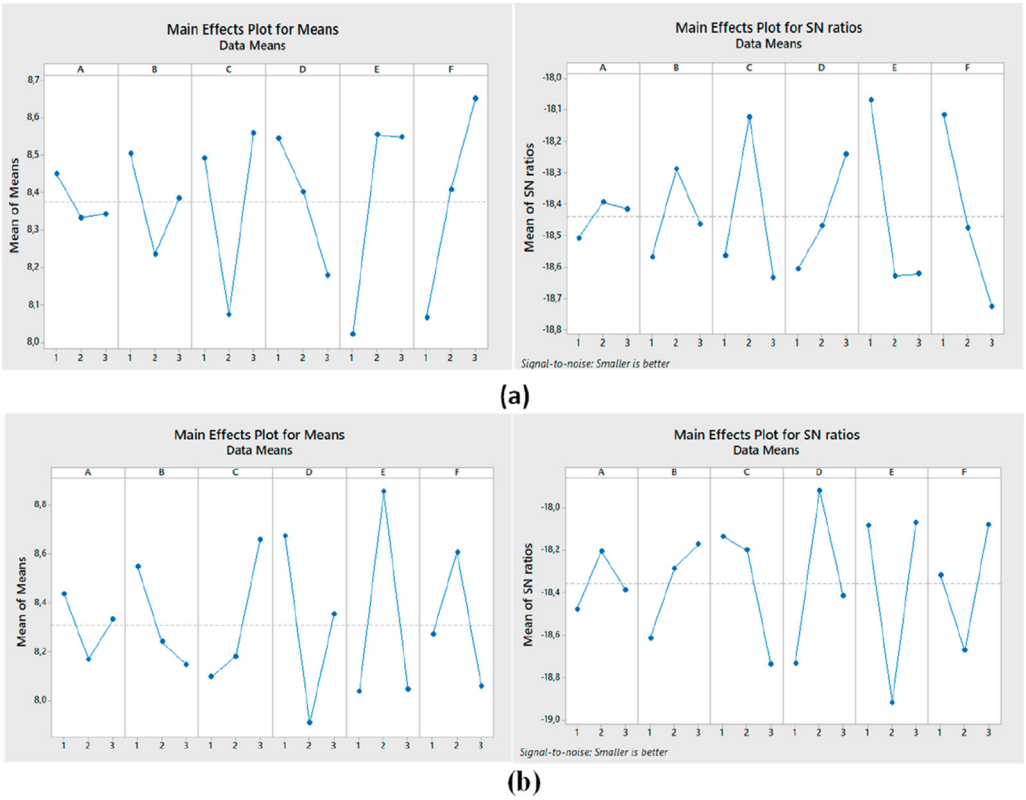

Figure 4. Plots of mean Ra and S/N ratios of insoles for two patients with diabetes: (a) left foot; (b) right foot.

3.1. Analysis of the S/N ratio

The Ra values were obtained from the experiments with the different cutting parameters, and the results are presented in Table 3. Each factor level corresponding to the quality features was examined using the S/N ratio. It can be seen that a low Ra value could be achieved with the optimal machining conditions. In this case, the cutting parameters and their levels for the machining of the left-foot insoles were related to the second level of the toolpath strategy (A), depth of cut (D), and typical design of insoles (F); the first level of the feed rate (C) and hardness of EVA foam (E); and the third level of the spindle speed (B). For the Ra value of the right-foot insoles, the levels of machining for the target value corresponded to level 2 of the tool path strategy (A), spindle speed (B), feed rate (C), depth of cut (D), and typical design of the insole (F), and level 1 of the hardness of EVA foam (E). Therefore, two conditions of the optimal cutting parameters yielding the minimum surface roughness Ra were simplified as follows: $A_2B_3C_1D_2E_1F_2$ (left-foot insoles) and $A_2B_2C_2D_2E_1F_2$ (right-foot insoles) (Figure 4).

Figures 4(a) and 4(b) show the S/N ratio results of the optimal parameter settings for Patient 1 and Patient 2, respectively, with the S/N ratios for the six parameter settings. Here, each optimal parameter setting has a minimal S/N ratio tendency. The optimal Ra value is proportional to the minimum S/N ratio. The selected scenario is the STB because the optimal Ra was obtained with the minimum S/N ratio. This indicates that the quality of the parameters was optimal with the minimum Ra.

3.2. TM-based selection of the optimal cutting condition

The interaction analysis in the S/N ratios showed that $A_2B_3C_1D_2E_1F_2$ and $A_2B_2C_2D_2E_1F_2$ are the optimal combinations for yielding low Ra values (left- and right-foot insoles). For the machining of the left-foot insole, two parameters in the S/N data analysis were found to be significant: feed rate and surface hardness materials. Lower feed rates and surface hardness are preferred for achieving the minimum Ra for the left-foot insoles. Likewise, milling the low-hardness EVA foam helps realize the minimum Ra for the right-foot insoles. Therefore, the predicted optimal surface roughness (Ra_{pred}) of the left-foot insole can be expressed as follows:

$$Ra_{pred} = T_{Ra\_exp} + \left(\overline{A}_2 - T_{Ra\_exp}\right) + \left(\overline{B}_3 - T_{Ra\_exp}\right) + \left(\overline{C}_1 - T_{Ra\_exp}\right) + \left(\overline{D}_2 - T_{Ra\_exp}\right) + \left(\overline{E}_1 - T_{Ra\_exp}\right) + \left(\overline{F}_2 - T_{Ra\_exp}\right), \quad (5)$$

where $\overline{T}_{Ra\_exp} = 8.3742$, $\overline{A}_2 = 8.332$, $\overline{B}_2 = 8.384$, $C_1 = 8.492$, $\overline{D}_2 = 8.178$, $\overline{E}_1 = 8.020$, and $\overline{F}_2 = 8.064$; hence, Ra_{pred} (left-foot insole) = 8.3742 + (8.332–8.3742) + (8.384–8.3742) + (8.492–8.3742) + (8.178–8.3742) + (8.020–8.3742) + (8.064–8.3742) = 7.599 μm. Likewise, the predicted optimal surface roughness (Ra_{pred}) of the right-foot insole can be expressed as follows:

$$Ra_{pred} = T_{Ra\_exp} + \left(\overline{A}_2 - T_{Ra\_exp}\right) + \left(\overline{B}_3 - T_{Ra\_exp}\right) + \left(\overline{C}_1 - T_{Ra\_exp}\right) + \left(\overline{D}_2 - T_{Ra\_exp}\right) + \left(\overline{E}_1 - T_{Ra\_exp}\right) + \left(\overline{F}_2 - T_{Ra\_exp}\right), \quad (6)$$

where $T_{Ra\_Exp} = 8.3106$, $\overline{A}_2 = 8.16$, $\overline{B}_3 = 8.146$, $C_1 = 8.096$, $\overline{D}_2 = 7.907$, $\overline{E}_1 = 8.044$, and $\overline{F}_2 = 8.057$; hence, Ra_{pred} (left-foot insole) = 8.3106 + (8.168–8.3106) + (8.146–8.3106) + (8.096–8.3106) + (7.907–8.3106) + (8.044–8.3106) + (8.057–8.3106) = 6.865 μm.

The confidence interval (CI), which was considered to predict the optimal values, can be calculated as follows (Roy, 1990):

$$CI = \sqrt{F_{\alpha,dofV_{error}} V_{error} x \left(\frac{1}{n_{eff}}\right)}, \quad (7)$$

$$n_{eff} = \frac{\text{Number of experiment}}{1 + \text{total dof in items in used in estimate}}. \quad (8)$$

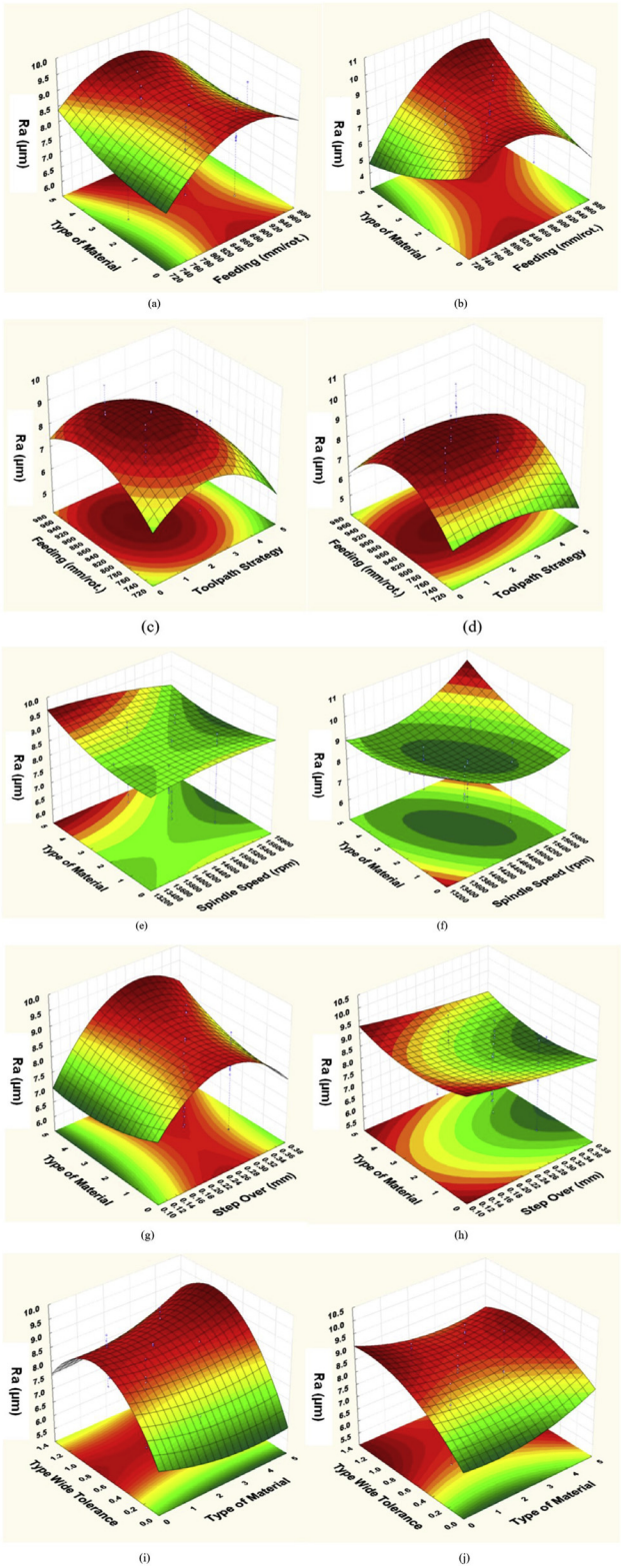

Figure 5. 3D plot of the surface roughness of the insoles: (a) material vs. feed rate for left foot; (b) material vs. feed rate for right foot; (c) feed rate vs. toolpath strategy for left foot; (d) feed rate vs. toolpath strategy for right foot; (e) material vs. spindle speed for left foot; (f) material vs. spindle speed for right foot; (g) material vs. step over for left foot; (h) material vs. step over for right foot; (i) width tolerance vs. material for left foot; (k) width tolerance vs. material for right foot.

The confidence intervals of the surface roughness Ra_{pred} for the left-foot insole was calculated to be $CI_{Ra} = \pm\ 0.652$ µm using the following parameters: $F_{0.05;1.26} = 4.23$ (tabulated), $V_{erorr} = 0.2259$ (Table 5), $N_{eff} = 2.25$, and $CI_{Ra} = \pm\ 0.652$ µm. The predictive mean of Ra_{pred} was found to be 7.599 µm. $|Ra_{pred} - CI| < Ra_{pred} < |Ra_{pred} + CI|$; thus, 7.599–0.652 µm < 7.599 µm $< 7.599 + 0.652$ µm and 6.947 µm $< Ra_{pred} < 8.251$ µm.

The confidence interval of the surface roughness Ra_{pred} for the right-foot insole was calculated to be $CI_{Ra} = 0.625$ µm using the following parameters: $F_{0.05;1.26} = 4.23$ (tabulated), $V_{erorr} = 0.208$ (Table 5). a), and $N_{eff} = 2.25$. The predictive mean of Ra_{pred} was found to be 6.865 µm. $|Ra_{pred} - CI| < Ra_{pred} < |Ra_{pred} + CI|$; thus, 6.865–0.625 µm < 6.865 µm $< 6.865 + 0.625$ µm and 6.127 µm $< Ra_{pred} < 7.377$ µm.

Table 5 presents the results of the experimental validation according to the optimal parameter combinations. The confidence intervals for the minimum Ra of the left- and right-foot insoles were calculated to be 0.652 and 0.625 µm, respectively. The results of the validation tests for the responses provided a CI value of 95%. In the CNC milling for the left-foot insole, the system optimization of Ra values was achieved using the smallest value of the feed rate and the relevant factor of the lowest surface hardness materials. This result is in good agreement with that of a previous study (Anggoro et al., 2016). Similarly, the smallest target value of surface roughness in the right-foot insole was obtained by machining EVA foam with the lowest surface hardness value.

3.3. ANOVA in the RSM

ANOVA was used to evaluate the significance of the regression model and individual model coefficients of the parameters (toolpath strategy, spindle speed, feed rate, step over, the type of EVA foam, and width of tolerance design) contributing to the surface roughness of the insoles. The ANOVA results for the surface roughness of the insoles are presented in Tables 6(a) and (b). The P-value and its percentage (%) contribution provided confidence to the significance level of all variables. The second regression model provided a P-value lower than 0.05, indicating that both models are statistically significant at a 95% confidence level. Moreover, the values of the contribution (%) for the response of the surface roughness of the left- and right-foot insoles are 80.90% and 88.63% with errors of 19.10% and 11.37%, respectively. The variation in these values indicates their degree of influence on the surface roughness values. For the left- and right-foot insoles, the parameter combination of D, E, F, C*C and C, D*D, E*E, respectively, interacting with BE parameters provided the optimal setting for the surface roughness values of the left-foot insole.

Further percentages of contribution to the linear and square models and interactions between parameters for the surface roughness values of the left-foot insole were 25.89% (linear), 21.74% (square), and 14.51% (interactions between factors). Here, D, E, and F contributed more significantly with percentages of 7.21%, 5.90%, and 6.89%, respectively, followed by factors A (0.61%), B (0.78%), and C (0.24%) (Table 6(a)). The surface roughness value of the right-foot insole was contributed by factors C (9.48%), B (4.87%), D (3.06%), E (035%), A (0.33%), and F (0.21%) (Table 6(b)). Correspondingly, the low value of the surface roughness of the insoles could be achieved by the optimal milling conditions (feed rate and type of material EVA foam), which is in close agreement with published works (Sarıkaya and Güllü, 2014; Anggoro et al., 2019a; Bawono et al., 2019; Chabbi et al., 2017; Asiltürk and Nesseli, 2012).

The combined two-factor interaction with the models after a single step calculation did not have a significant influence on a single parameter ($p > 0.05$). Accordingly, the next step to analyze the combined factors was focused on governing the interaction of obtaining $P < 0.05$. In this way, the interaction of several factors for the setting parameters could be simulated by the RSM, providing test parameter relationships in six parameter settings. Table 6 presents the interactions between the six factors, including linear (single), quadratic, and cubic interactions. The

Table 5. Comparisons of results of the experimental and TM-predicted values.

Response	Experimental result	Calculated value	Confidence interval (CI)	Difference $Ra_{exp} - Ra_{cal}$	Optimization
$Ra_{left\ foot}$ (μm)	$Ra_{exp} = 8.080$	$Ra_{cal} = 7.599$	$CI_{Ra} = 0.652$	0.481	0.418 < 0.652 Successful
$Ra_{rightfoot}$ (μm)	$Ra_{exp} = 7.476$	$Ra_{cal} = 6.865$	$CI_{Ra} = 0.625$	0.611	0.611 < 0.625 Successful

Table 6(a). ANOVA of the surface roughness Ra of the left-foot insole.

Source	DF	SS	MS	F-value	P-Value	Contribution %
Model	19	6.72428	0.35391	1.56	0.283	80.90
Linear	6	2.15206	0.35868	1.58	0.280	25.89
A	1	0.05088	0.05088	0.22	0.650	0.61
B	1	0.06468	0.06468	0.29	0.610	0.78
C	1	0.01987	0.01987	0.09	0.776	0.24
D	**1**	**0.59915**	**0.59915**	**2.64**	**0.0148**	**7.21**
E	**1**	**0.49070**	**0.49070**	**2.16**	**0.0185**	**5.90**
F	**1**	**0.57305**	**0.57305**	**2.53**	**0.0156**	**6.89**
Square	6	1.80677	0.30113	1.33	0.356	21.74
A*A	1	0.02419	0.02419	0.11	0.754	0.29
B*B	1	0.26586	0.26586	1.17	0.315	3.20
C*C	**1**	**1.23125**	**1,23125**	**5.43**	**0.053**	**14.81**
D*D	1	0.00992	0.00992	0.04	0.84	0.12
E*E	1	0.25812	0.25812	1.14	0.321	3.11
F*F	1	0.03781	0.03781	0.17	0.695	0.45
2-Way Interaction	7	1.20612	0.1723	0.76	0.637	14.51
A*E	1	0.03001	0.03001	0.13	0.727	0.36
A*F	1	0.01656	0.01656	0.07	0.795	0.20
B*E	**1**	**0.95718**	**0.95718**	**4.22**	**0.079**	**11.52**
B*F	1	0.07214	0.07214	0.32	0.590	0.87
C*E	1	0.01007	0.01007	0.04	0.839	0.12
C*F	1	0.6649	0.6649	2.93	0.131	8.00
D*E	1	0.4238	0.4238	1.87	0.214	5.10
Error	7	1.58759	0.2268			19.10
Total	26	8.31186				100

degree of influence can be determined from the contribution of the factors (% contribution) to the mathematical model of the minimum Ra value. A greater contribution value indicates a greater influence of the factor. From Table 6, it is evident that the contributions of factors E and F are 17.20% and 17.04%, respectively. This means that the influence of that factor E and F is approximately 17%.

3.4. RSM-based modeling for surface roughness

The RSM was employed for modeling and analyzing the dependent and independent variables of Ra in a specific range considering the experimental results of the CNC milling of the EVA foam. Furthermore, the second-order model of the surface roughness of the Ra could be generated as a function of the machining parameters (toolpath strategy, spindle speed, feed rate, and step over). The relationship between the surface roughness Ra and the milling parameters in this study can be expressed as follows [Eq. (9)]:

Accordingly, a mathematical model of the surface roughness can be generated using the results of optimized milling parameters (A, B, C, D, E, and F). According to the RSM, the surface roughness Ra models can be expressed s follows [Eqs. (9) and (10)]:

$$R_a = \beta_0 + \beta_1.A + \beta_2.B + \beta_3.C + \beta_4.D + \beta_5.E + \beta_6.F + \beta_7.A.B + \beta_8 A.C + \beta_9 A.D + \beta_{10} A.E + \beta_{11} A.F + \beta_{12} B.C + \beta_{13} B.D + \beta_{14} B.E + \beta_{15} B.F + \beta_{16} C.D + \beta_{17}.C.E + \beta_{18} C.F + \beta_{19} D.E + \beta_{20} D.F + \beta_{21} E.F + \beta_{22} A^2 + \beta_{23}.B^2 + \beta_{24} C^2 + \beta_{25} D^2 + \beta_{26} E^2 + \beta_{27} F^2. \quad (9)$$

Table 6(b). ANOVA of surface roughness Ra of the right-foot insole.

Source	DF	SS	MS	F-value	P-Value	Contribution
						%
Model	19	13,2326	0,69645	2,87	0,079	88,63
Linear	6	2,7166	0,45276	1,87	0,216	18,20
A	1	0,0498	0,04982	0,21	0,664	0,33
B	1	0,7272	0,72722	3	0,127	4,87
C	**1**	**1,4151**	**1,41512**	**5,84**	**0,046**	**9,48**
D	1	0,4563	0,45633	1,88	0,212	3,06
E	1	0,0528	0,05282	0,22	0,655	0,35
F	1	0,0313	0,03133	0,13	0,73	0,21
Square	6	6,688	1,11467	4,6	0,033	44,80
A*A	1	0,2761	0,27606	1,14	0,321	1,85
B*B	1	0,0709	0,07085	0,29	0,606	0,47
C*C	1	0,2348	0,23483	0,97	0,358	1,57
D*D	**1**	**2,2034**	**2,20342**	**9,09**	**0,02**	**14,76**
E*E	**1**	**3,532**	**3,53204**	**14,56**	**0,007**	**23,66**
F*F	1	0,7041	0,70409	2,9	0,132	4,72
2-Way Interaction	7	2,4444	0,3492	1,44	0,321	16,37
A*E	1	0,0397	0,03967	0,16	0,698	0,27
A*F	1	0,0927	0,09274	0,38	0,556	0,62
B*E	**1**	**1,3092**	**1,30918**	**5,4**	**0,053**	**8,77**
B*F	1	0,7116	0,71162	2,93	0,13	4,77
C*E	1	0,8467	0,84666	3,49	0,104	5,67
C*F	1	0,6844	0,68445	2,82	0,137	4,58
D*E	1	0,1929	0,19287	0,8	0,402	1,29
Error	7	1,6976	0,24252			11,37
Total	26	14,9302				100,00

Table 7. Optimal parameters and validation results of the experimental and RSM-predicted values.

Optimal Cutting Parameter Conditions	Toolpath	Spindle Speed	Feed Rate	Step Over	Type of EVA Rubber Foam	Width Tolerance	Surface Roughness Ra		Percentage Error (%)
		(RPM)	(mm/min)	mm	(HRC)	(mm)	Exp.	RSM	
							μm		
$\mathbf{A_2B_2C_2D_2E_1F_2}$	*raster 45*	14,500	850	0.25	20–35	0.75	**8.080**	8.160	0.98
$\mathbf{A_2B_3C_1D_2E_1F_2}$	*raster 45*	14,500	850	0.25	20–35	0.75	**7.476**	7.672	**2.56**

$$Ra_{right\_foot} = 9.78 - 1.386A - 0.693B - 0.417C - 3.022D + 1.45E + 2.81F + 0.215A^2 + 0.109B^2 + 0.198C^2 + 0.606D^2 - 0.886E^2 - 0.396F^2 + 0.094AE + 0.144AF + 0.426BE - 0.398BF + 0.343CE - .390CF + 0.220DE \quad (11)$$

roughness are presented in Figure 5. In the machining of the right-foot insole, the minimum surface roughness could be achieved when selecting the EVA foam with the lowest surface hardness, middle level of spindle speed, and high levels of toolpath strategy and step over. In

$$Ra_{left\_foot} = 7.68 - 0.023A - 0.426B - 2.473C + 0.631D + 2.81E - 0.28F + 0.064A^2 + 0.211B^2 + 0.453C^2 - 0.041D^2 - 0.240E^2 - 0.092F^2 - 0.082AE - 0.061AF - 0.365BE + 0.127BF - 0.037CE + 0.384CF - 0.325DE \quad (10)$$

Eqs. (10) and (11) were subsequently used for the determination of R^2. The responses for the surface roughness values of the left- and right-foot insoles yielded R^2 values of 90.90% and 98.63%, respectively, which are suitable for this experiment. Therefore, the above models can be used to predict the response of the surface roughness at specific design parameters.

Further parameter interactions among machining variables contributing to the surface roughness values can be predicted from the 3D-plots of the RSM models (Eqs. (10) and (11)). The 3D-plots for the relationship between the cutting parameters and the response of the surface

contrast, the minimum surface roughness of the left-foot insole was achieved when selecting low feed rate, spindle speed, toolpath strategy, and step over, and did not depend on the level of surface hardness of the EVA foam. From these results, the increasing feed rate during the machining process generated vibration and heat, contributing to the higher surface roughness (Yadav, 2017). The lowest step over resulted in a reduction in the surface roughness value. Figure 5(e) shows the relationship between the width tolerance, surface hardness of the material, and surface roughness of both insoles. It can be seen that the lowest width tolerance of insoles corresponded to the minimum surface roughness.

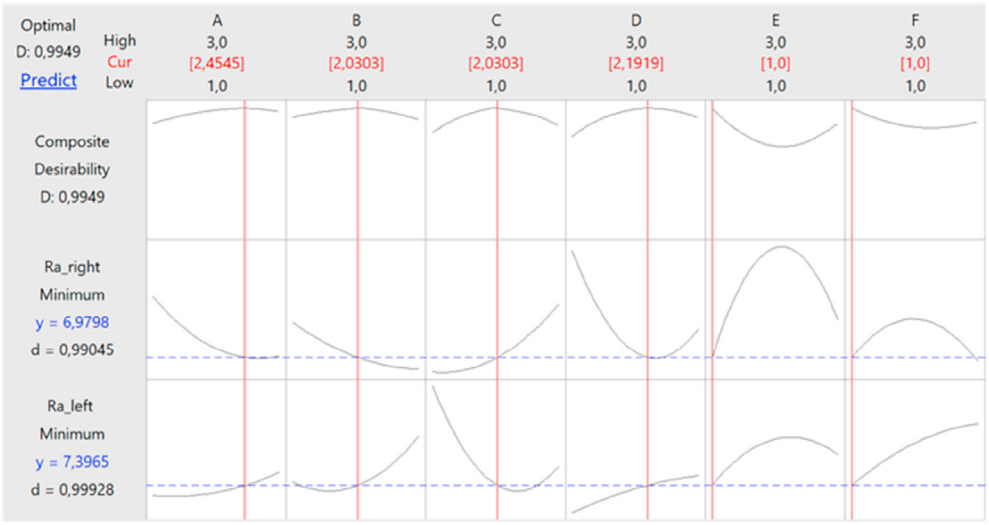

Figure 6. Optimized result obtained with the TM-RSM (D = composite desirability; d = individual desirability; High = highest value parameter; Cur = optimal current value of control parameter; Low = lowest value parameter, y = response parameter, Ra = average surface roughness; A = toolpath strategy; B = spindle speed; C = feed rate; D = step over; E = EVA foams with variable hardness; F = typical design of insoles with wider tolerance).

Table 8. Comparison of the optimal and predicted results.

Optimization technique	Ra				Absolute error (%)	
	Optimal		Predicted			
	Left Foot (μm)	Right Foot (μm)	Left Foot (μm)	Right Foot (μm)	Left Foot	Right Foot
TM	8.080	7.476	7.599	6.865	5.95	8.17
TM-RSM	7.397	6.980	8.160	7.672	**10.32**	**9.91**
Percentage improvement (%)	**9.23**	**7.11**	-	-		

With the developed model, the Ra values of the left- and right-foot insoles were predicted to be 8.538 and 7.828 μm, respectively. These values were predicted with a toolpath strategy of raster 450, spindle speed of 14,500 rpm, feed rate of 850 mm/min, and step over of about 0.25 mm. The EVA foam with a surface hardness of 20–35 HRC (Level 1) allowed the design of insoles with wider tolerances of 0.75 mm. Under these conditions, the predicted values have a similar trend as the experimental values in the CNC milling with absolute average percentage errors for both insoles of less than 3.6% (Table 7). The results of the proposed model are consistent with those of previous studies (Hanafi et al., 2012; Asiltürk and Nesseli, 2012; Sarıkaya and Güllü, 2014).

Ra was determined considering the STB criteria for the surface quality. The Ra value of 10 μm is generally considered as "the best" (Anggoro et al., 2017, 2018, 2019a, 2019c). Accordingly, the obtained Ra values ranging from 7 to 9 μm are acceptable. Moreover, the EVA foam with surface hardness ranging from 20 to 35 HRC is the most appropriate for the insoles of AFO shoes, which are often used as a semi-rigid insole (Janisse and Janisse, 2006). In the present study, the CNC milling of EVA foam with varying hardness provided a high surface

Figure 7. Set up for the test of the AFO shoes in two patients.

Figure 8. CARES design of AFO shoe.

roughness in the range of 7–9 μm; in the process, small pieces of foam were produced owing to the flutes of the ball-nose cutter, which leads to material wastage. In terms of economic value, the use of EVA foam with a size of 1200 × 2400 × 30 mm^3 (price $31/sheet) for insoles provided the lowest-cost product. Hence, the EVA foam with low hardness and low cost is desirable for the best level and the best typical design of insoles with wider tolerance.

3.5. Optimization using desirability function analysis with TM-RSM

The predicted responses were analyzed and subsequently converted into a desirability value (dF) (Sait et al., 2009) between 0 and 1, with 0 indicating a completely unacceptable response and 1 indicating a perfect response. In this study, the desirability function was selected following the STB criterion because the minimum surface roughness was achieved at the optimal process parameters. Figure 6 shows the analysis results of the composite desirability (D) and the optimal response corresponding to each control parameter.

The predicted optimal Ra of the left-foot insole is 7.3965 μm; this was obtained at a factor A, B, C, D, E, and F of level 2.4545, 2.0303, 2.303, 2.1919, 1, and 1, respectively. In contrast, the predicted optimal Ra of the right-foot insole is 6.9798 μm; this was obtained at a factor A, B, C, D, E, and F of level 2.4545, 2.0303, 2.303, 2.1919, 1, and 1, respectively. Moreover, the desirability values for left- and right-foot insoles are 0.99928 and 0.99045, respectively; hence the desirability Ra value is close to 1.0. Consequently, the response is considered perfect for the target value.

Validation tests were performed to predict the optimal conditions and the experimental results of the responses (Ra = 8.080 μm and 7.476 μm for the left- and right-foot insoles, respectively) (Table 7). The predictive ability of the established model was verified in the optimal condition, in which the predicted Ra values of 8.160 and 7.672 μm for the left- and right-foot insoles, respectively, were suitable for the model (Tables 6 and 7). The optimal outcomes of the surface quality products obtained by different optimization methods (TM and RSM) were then significantly enhanced by the hybrid TM-RSM. The optimal results predicted and obtained through the analysis are summarized in Table 8. It can be seen that the use of the hybrid TM-RSM leads to a surface quality of the left- and right-foot insoles 9.23% and 7.11% higher than the TM, respectively; the prediction ability of the TM-RSM is significant at 10.32% and 9.91% errors, respectively, at the optimal condition.

3.6. Proposed machining strategy of ankle-foot orthotic (AFO) shoes

AFO shoes are designed specifically for patients with foot deformities and diabetes (Telfer and Woodburn, 2010; Anggoro et al., 2018, 2019b). In this study, the AFO shoe were tested on two diabetic patients more than 60 years old walking on a flat surface condition (Figure 7), as shown in Figure 3 (c). A computer-aided reverse engineering system (CARES) was used to accurately fit the AFO insoles to patient's feet (Figure 8).

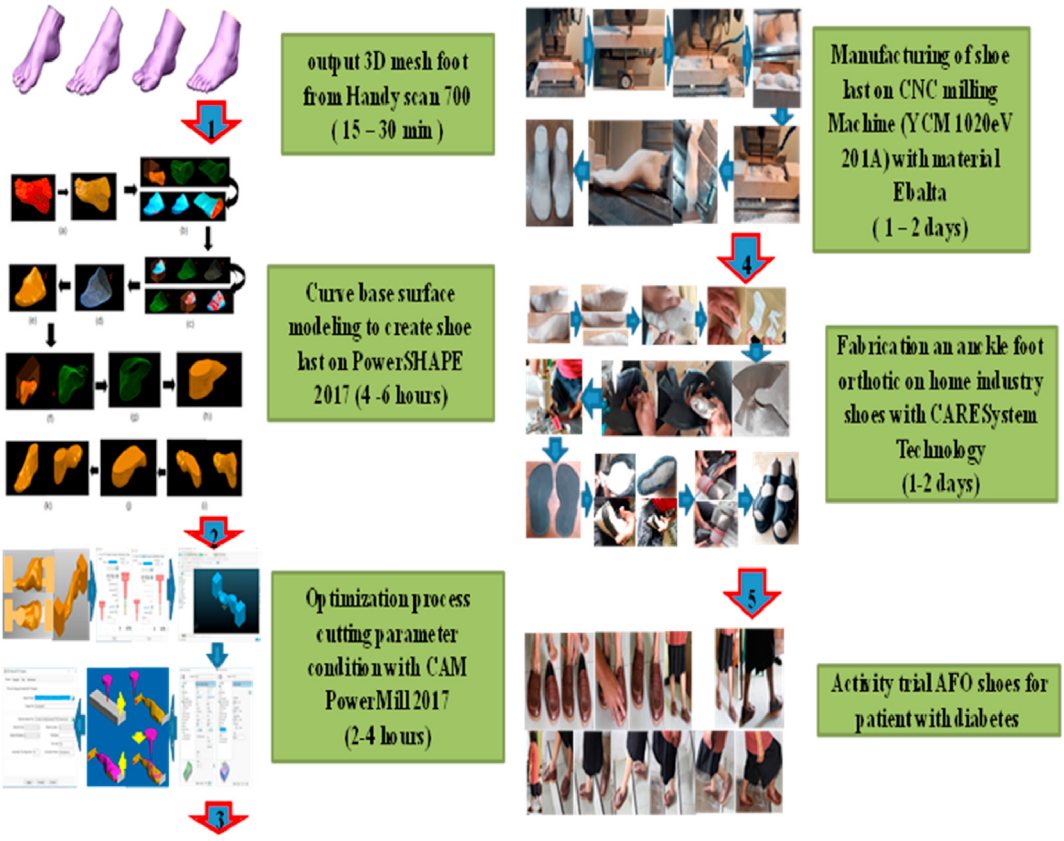

Figure 9. Manufacturing stages of AFO shoes.

CARESs solve the problem of the reduction of pain due to the use of general shoes or difficulty in carrying out daily activities experienced by patients with a deformed foot (Anggoro et al., 2018, 2019b, 2019c).

The initial stages of the design, manufacturing, and fabrication of the AFO shoes began by 3D printing with the scanning tool Handyscann 700™ to obtain a wide fit tolerance and precision of the foot. For this purpose, the design process of the insoles could be fully explored by modeling the surface base (Ye et al., 2008; Chabbi et al., 2017; Anggoro et al., 2018, 2019b; Bawono et al., 2019), while the 3D CAD model of the insole and shoe last orthotic shoes could be retrieved directly for manufacturing processes in CNC machines. In this study, the quality of the insole surface and the machining time were estimated using the PowerMILL CAM software with the machining parameters in accordance with the obtained condition of the TM-RSM. Two types of CNC machines (Rolland Modela 40R and YCM EV1020A) were used to obtain shoe components from Ebalta wood (see Figure 8). The proposed stages of the AFO CARES-based system are shown in Figure 9.

The AFO insole shoes were fabricated in 108.5 h, which is 64% faster than the time required by traditional methods (almost two months) (Anggoro et al., 2019b). The significant finding of the study may be the fabrication of a proper shoe fit for patients with foot disorders (Figure 7), in which diabetic patients generally experience a disruption in their feet. This foot disorder is related to stabbing pain when the patient performs activities. The two diabetic patients wore the AFO shoes for 28 days (4 weeks). At the end of the period, each patient was prompted to answer a questionnaire of 16 questions, which were divided according to the Manchester–Oxford Foot Questionnaire (MOXFQ). The response was measured by a score of 0–4 (strongly agree to strongly disagree). The respondents were two female patients aged 65 and 80 years, hereafter referred to as P1 and P2, respectively, who responded independently to the questionnaire. The MOXFQ was examined to determine the pain associated with wearing the AFO shoes for 2 months. P1 reported an improvement in the conditions of the base with a scoring average of 3.75 (12/16 answers with the scores of 4 or 3). A 94% decrease in pain was reported by P1. Conversely, P2, who had repaired her foot, gave an average score of 2.97. She reported a reduction in pain of 74%. The different results may be related to the characteristics of the age, weight, height, and profile of the soles of the feet (Bawono et al., 2018).

Further testing of the AFO product in both patients using the AFO footwear successfully decreased the level of pain. A value of 0 indicates that the patient felt pain, and a value of 4 indicates that the patient did not feel pain. P1 gave scores of 4 (12 questions) or 3 (4 questions) with an average 3.75 (maximum scale 4), indicating that he did not feel pain (four answers concerned the pain that was experienced in both legs especially when she was standing too long, taking the car, and doing recreational activities). P2 gave scores of 4 (4 questions) or 3 (10 questions), with an average of 2.97, indicating that she felt pain, especially when she stood for too long and during walking and running. The different levels of pain may be due to the difference in age. However, both P1 and P2 reported a reduction in the pain while wearing the AFO shoes. The result indicated that 94% and 74% of the pain in P1 and P2 disappear, and only about 2% of the pain remained in certain activities (albeit, this occurred rarely).

4. Conclusions

The hybrid TM-RSM was applied for the modeling and optimization of the CNC milling of EVA foam for orthotic shoe insoles. The results of this research can be summarized as follows:

1. The 3D surface roughness plots illustrate the synergistic effects of the hardness in the EVA foam and the feed rate, step over, spindle speed,

and tool path on the yields of surface roughness. With the hybrid TM-RSM, the following optimal machining parameter combinations were found: raster toolpath strategy of 450 and step and shallow machining; spindle speed of 14500 rpm, feed rate of 850 mm/min; step over of approximately 0.25 mm; surface hardness of EVA foam of 20–35 HRC; width tolerance of 0.75 mm. With these optimal parameters, the optimal Ra for the left- and right-foot insoles were found to be 7.397 and 6.980 μm, respectively. Moreover, the surface quality obtained with the hybrid method was higher than that obtained with the TM (9.23% and 7.11% higher for the left- and right-foot insoles). EVA rubber foam with a surface hardness of 20–35 HRC was proposed for suitable material insoles that can be manufactured through CNC milling. Correspondingly, both the TM and TM-RSM may be applied to optimize the input data in milling operations of AFO shoe insoles with shorter fabrication time and price.

2. Results of designing on the insole, outsole, and shoe orthotics with existing CAD software provided the AFO's new product trials in both patients by savings of the entire production process approximately 64%. The AFO shoes exhibited highly accurate surface contours and wide dimensional tolerance fits for the patients' feet, and also provided a good level of comfort and reduced pain in patients. In future studies, the hybrid TM-RSM and CARES will be applied for the advanced design and manufacturing of custom AFO shoes for disabled patients (e.g., patients with flat feet, high-heel syndrome, Morton's neuroma syndrome, metatarsalgia, and club foot). This scheme is expected to solve the custom design and manufacturing problems faced by sandals and shoe producers in developing customized AFO products.

Declarations

Author contribution statement

P.W. Anggoro: Conceived and designed the experiments; Analyzed and interpreted the data; Wrote the paper.

B. Bawono: Performed the experiments.

J. Jamari: Analyzed and interpreted the data.

A.P. Bayuseno: Contributed reagents, materials, analysis tools or data; Wrote the paper.

M. Tauviqirrahman: Conceived and designed the experiments; Wrote the paper.

Funding statement

This research by Directorate of Research and Community Service, Directorate General of Research and Development Strengthening, Ministry of Research, Technology and Higher Education Fiscal Year 2019, grant Number: 257-93/UN7.P4.3/PP/2019 and Number: 257-73/UN7.P4.3/PP/2019 and Letter of agreement for the implementation of research acceleration grants at the Atma Jaya University Yogyakarta, Number: 382/HB - PEN PGB/LPPM/XI/2019.

Competing interest statement

The authors declare no conflict of interest.

Additional information

No additional information is available for this paper.

Acknowledgements

We would like to gratefully thank the Directorate of Research and Community Service, Directorate General of Research and Development Strengthening, Ministry of Research, Technology and Higher Education Fiscal Year 2019–2021, PUTP Polytechnic ATMI Surakarta, Tribology Laboratory of the Department of Mechanical Engineering, University of Diponegoro in Semarang, and CV Sibad Engineering Semarang for full support with the CAD, CAM, CNC and reverse engineering during the design, developed process, and help with the writing of this paper.

References

Anggoro, P.W., Bawono, B., Jamari, J., Bayuseno, A.P., 2016. Parameter Optimization of strategies at CNC Milling Rolland Modela MDX 40R CAM made insole shoe orthotic EVA foam. Int. J. Mechatron. Mech. Eng. 6, 96–106.

Anggoro, P.W., Saputra, E., Tauviqirrahman, M., Jamari, J., Bayuseno, A.P., 2017. A 3-dimensional finite element analysis of the insole shoe orthotic for foot deformities. Int. J. Appl. Eng. Res. 5 (1), 5254–5260.

Anggoro, P.W., Tauviqirrahman, M., Jamari, J., Bayuseno, A.P., Bawono, B., Avellina, M.M., 2018. Computer-aided reverse engineering system in the design and production of orthotic insole shoes for Patients with diabetes. Cogent Eng. 5 (1), 1–20.

Anggoro, P.W., Bawono, B., Tauviqirrahman, M., Jamari, J., Bayuseno, A.P., Wicaksono, A., 2019a. Reverse innovative design of insole shoe orthotic for diabetic patients. J. Eng. Appl. Sci. 14 (1), 106–113.

Anggoro, P.W., Tauviqirrahman, M., Jamari, J., Bayuseno, A.P., Wibowo, J., Saputro, Y.D., 2019b. The Optimal design and manufacturing of shoe last product for an ankle-foot orthotic for the patient with diabetes. Int. J. Manuf. Mater. Mech. Eng. 9 (issue 2), 62–80.

Anggoro, P.W., Bawono, B., Tauviqirrahman, M., Jamari, J., Bayuseno, A.P., 2019c. Design and manufacturing orthotics shoe insole with optimum surface roughness using the cnc milling. J. Eng. Sci. Technol. 14 (issue 4), 1799–1819.

Asiltürk, I., Nesseli, S., 2012. The multiresponse optimization of CNC turning parameters with Taguchi method-based response surface analysis. Measurement 45, 785–794.

Bawono, B., Anggoro, P.W., Tauviqirrahman, M., Jamari, J., Bayuseno, A.P., 2018. The evaluation of the use of AFO (ankle foot orthotics) with the MOXFQ (Manchester-Oxford foot questionnaire) method, atlantis highlights in engineering (AHE). 1, 657 – 662. In: International Joint Conference of Science and Technology (IJCST 2018).

Bawono, B., Anggoro, P.W., Tauviqirrahman, M., Jamari, J., Bayuseno, A.P., 2019. Milling strategy optimized for orthotics insole to enhance surface roughness and machining time by Taguchi and response surface methodology. J. Indus. Prod. Eng. 36 (4), 1–20.

Berry, C., Wang, H., Jack Hu, S., 2013. Product architecture for personalization. JMSY 32, 404–411.

Boulton, A.J., Krasner, R.S., Vileikyte, L., 2004. Clinical practice. Neuropathic diabetic foot ulcers. N. Engl. J. Med. 351, 48–55.

Chabbi, A., Mabrouki, T., Yallese, M.A., Nouioua, M., Meddour, I., 2017. Modeling and optimization of turning process parameters during the cutting of polymer (POM C) based on RSM, ANN, and DF methods. Int. J. Adv. Manufact. Technol. 43, 581–589.

Creylman, V., Muraru, L., Pallari, J., Vertomen, H., Peeraer, L., 2013. Gait assessment during the initial fitting of customized selective laser sintering ankle-foot orthoses in subjects with drop foot. Prosthet. Orthot. Int. 37 (2), 32–1388.

Dombroski, C.E., Froats, A., Balsdon, M.E.R., 2014. The use of a low cost 3D scanning and printing tool in the manufacture of custom-made foot orthoses: a preliminary study. BMC Res. Notes 7, 443–447.

Faustini, M.C., Stanhope, S.J., Crawford, R.H., Neptune, R.R., 2008. The manufacture of passive dynamic ankle-foot orthoses using selective laser sintering. IEEE Trans. Biomed. Eng. 55 (2 Pt 1), 784–790.

Ghassemi, A., Karimi, M.T., Mossayebi, A.R., Jamshidi, N., Naemi, R., 2015. Manufacturing and finite element assessment of a novel pressure reducing insole for Diabetic Neuropathic patients. Austral. Phys. Eng. Sci. Med. 38, 63–70.

Hanafi, I., Almansa, E., Khamlichi, A., Jabbouri, A., Cabrera, F.M., 2012. Optimization of cutting conditions for sustainable machining of PEEK-CF0 using TiN tools. J. Clean. Prod. 33, 1–9.

Hawke, F., du Toit, V., Burns, J., Radford, J.A., 2008. Custom-made foot orthoses for the treatment of foot pain (Review). Cochrane Database Syst. Rev. (3), CD006801, 2008 Jul 16 Published by John Wiley & Sons, Ltd. (2008).

Janisse, E.J., Janisse, D.J., 2006. Pedorthic and orthotic management of the diabetic foot. Foot Ankle Clin. N. Am. 11, 717–734.

Jeng, Y.R., Yau, H.T., Liu, D.S., 2012. Designing experimental methods to predict the expansion ratio of EVA foam material and using finite element simulation to estimate the shoe expansion shape. Mater. Trans. 53, 685–1688.

Landorf, K., Keenan, A.M., Rushworth, R.L., 2001. Foot orthosis prescription habits of australian and New Zealand podiatric physicians. J. Am. Podiatr. Med. Assoc. 91, 74–183.

Li, Y., Falk, B., Linke, B.S., Voet, H., Schmitt, R., Lam, M., 2017. Cost, sustainability and surface roughness quality – a comprehensive analysis of products made with personal 3D printers. CIRP-JMST. 16, 1–11.

Matricali, G.A., Mathieu, C., Dereymaeker, G., Muls, E., Flour, M., 2007. Economic aspects of diabetic foot care in a multidisciplinary setting: a review. Diabetes Metab. Res. Rev. 23, 339–347.

Montgomery, D.C., 2013. Design Analysis of Experiments, eighth ed. John Wiley & Sons, New York, USA.

Munro, W., 2005. Orthotic prescription process for the diabetic foot. Diabet. Foot 8, 72–82.

Myers, R.H., Montgomery, D.C., Anderson-Cook, C.M., 2009. Process and Product Optimization Using Designed Experiments, third ed. John Wiley & Sons, New York, USA.

Nurit, E.T., Ety, W., Yifat, H.F., Amit, G., 2006. Role of EVA viscoelastic properties in the protective performance of a sport shoe: computational studies. J. Bio-Med. Mater. Eng. 16, 289–299.
Pallari, J., Dalgarn, K.W., Woodburn, J., 2010. Mass customization of foot orthoses for rheumatoid arthritis using selective laser sintering. IEEE Trans. Biomed. Eng. 57, 1750–1756.
Qiu, T.X., Teo, E.C., Yan, Y.B., Lei, W., 2011. Finite element modeling of a 3D coupled foot-boot model. Med. Eng. Phys. 33, 228–1237.
Roy, R.K., 1990. A Primer on the Taguchi Method. Van Nostrand Reinhold, New York, USA.
Sait, A.N., Aravindan, S., Haq, A.N., 2009. Optimization of machining parameters of glass fiber-reinforce plastics analysis using the Taguchi technique. Int. J. Adv. Manuf. Technol. 43, 581–589.
Salles, A.S., Gyi, D.E., 2012. The specification of personalized insoles using additive manufacturing. Work 41 (suppl 1), 1771–1774.
Salles, A.S., Gyi, D.E., 2013. An evaluation of personalized insoles developed using additive manufacturing. J. Sports Sci. 31, 442–450.
Sarıkaya, M., Güllü, A., 2014. Taguchi design and response surface methodology based analysis of machining parameters in CNC turning under MQL. J. Clean. Prod. 65, 604–616.
Schrank, E.S., Stanhope, S.J., Hitch, L., Wallace, K., Moore, R., 2013. Assessment of a virtual functional prototyping process for the rapid manufacture of passive-dynamic ankle-foot orthoses. J. Biomech. Eng. 135, 101011–101017.
Shimazaki, Y., Inoue, T., Nozu, S., 2016. Shock-absorption properties of functionally graded EVA laminates for footwear design. Polym. Test. 54, 98–103.
Telfer, S., Woodburn, J., 2010. The use of 3D surface scanning for the measurement and assessment of the human foot. J. Foot Ankle Res. 3 (1), 1–9.
Vicenzino, B., 2004. Foot orthotics in the treatment of lower limb conditions: a musculoskeletal physiotherapy perspective. Man. Ther. 9, 185–192.
Xavior, M.A., Adithan, M., 2009. Determining the influence of cutting fluids on tool wear and surface roughness during turning of AISI 304 austenitic stainless steel. J. Mater. Process. Technol. 209, 900–909.
Xia, Z., 2014. Application of reverse engineering based on computer in product design. Int. J. Multimed. Ubiquitous Eng. 9, 343–353.
Yadav, R.N., 2017. A hybrid approach of Taguchi-RSM for modeling and optimization of duplex turning process. Measurement 100, 131–138.
Ye, X., Liu, H., Chen, L., Chen, Z., Pan, X., Zhang, S., 2008. Reverse innovative design- an integrated product design methodology. Comput. Aided Des. 40, 812–820.